

miR-483-5p Promotes Invasion and Metastasis of Lung Adenocarcinoma by Targeting RhoGDI1 and ALCAM

Qiancheng Song¹, Yuanfei Xu¹, Cuilan Yang¹, Zhenguo Chen¹, Chunhong Jia¹, Juan Chen¹, Yue Zhang¹, Pinglin Lai¹, Xiaorong Fan¹, Xuan Zhou¹, Jun Lin¹, Ming Li¹, Wenli Ma², Shenqiu Luo¹, and Xiaochun Bai¹

Abstract

The nodal regulatory properties of microRNAs (miRNA) in metastatic cancer may offer new targets for therapeutic control. Here, we report that upregulation of miR-483-5p is correlated with the progression of human lung adenocarcinoma. miR-483-5p promotes the epithelial–mesenchymal transition (EMT) accompanied by invasive and metastatic properties of lung adenocarcinoma. Mechanistically, miR-483-5p is activated by the WNT/ β -catenin signaling pathway and exerts its prometastatic function by directly targeting the Rho GDP dissociation inhibitor alpha (RhoGDI1) and activated leukocyte cell adhesion molecule (ALCAM), two putative metastasis suppressors. Furthermore, we found that downregulation of RhoGDI1 enhances expression of Snail, thereby promoting EMT. Importantly, miR-483-5p levels are positively correlated with β -catenin expression, but are negatively correlated with the levels of RhoGDI1 and ALCAM in human lung adenocarcinoma. Our findings reveal that miR-483-5p is a critical β -catenin–activated prometastatic miRNA and a negative regulator of the metastasis suppressors RhoGDI1 and ALCAM. *Cancer Res*; 74(11); 3031–42. ©2014 AACR.

Introduction

Tumor metastases are responsible for approximately 90% of all cancer-related deaths (1). Metastasis is a complex process by which cancer spreads from the place at which it first arose as a primary tumor to distant locations in the body. Metastasis depends on the cancer cells acquiring two separate abilities—increased motility and invasiveness (1). The epithelial–mesenchymal transition (EMT), a process in which epithelial cells lose their polarity and are converted into a mesenchymal phenotype, is regarded as a critical event during tumor metastasis (2, 3). The identification and characterization of molecules that control EMT, cell motility, and invasiveness are critical to our understanding of cancer dissemination. Critical regulators of the metastatic process include both proteins and microRNAs (miRNA).

WNTs and their downstream effectors regulate various processes that are important for cancer progression (4). Activation of Wnt/ β -catenin signaling in cancer often drives a transcriptional program such as transcriptional repressor of E-cadherin, Snail that is reminiscent of an EMT, which can promote cell migration and invasiveness (5). The dysregulation

of the Wnt/ β -catenin pathway has been observed in various forms of cancer. It has been recently shown that overexpression of WNTs and their downstream effectors are associated with poor prognosis in patients with non–small cell lung carcinoma (NSCLC) and involved in metastasis of lung cancer, the most common cause of cancer-related mortality worldwide (6–9). The mechanisms through which Wnt/ β -catenin regulates EMT and tumor metastasis, however, are currently not fully understood.

Another set of molecules that play crucial roles in metastasis are miRNA. miRNAs function as 21 to 24 nucleotide guides that regulate the expression of mRNAs containing complementary sequences. Studies have documented the role of miRNAs in the processes involved in metastasis, including cellular proliferation, migration and invasion, and EMT (10–12). The link between miRNAs and metastasis was first reported when miR-10b was shown to be involved in the promotion of breast cancer metastasis by direct targeting HOXD10 (13). This was followed by the discovery that miRNAs can also have a suppressive effect on metastasis, as increased mir-335 expression inhibited metastatic breast cancer cell invasion (14). More recently, several miRNAs such as miR-200, miR-205, and miR-221/222 have been shown to be involved in EMT (15, 16). Given that many miRNAs are deregulated in cancers but have not yet been further studied, it is expected that more miRNAs will emerge as critical players in the etiology and progression of cancer (17).

Recently, miR-483 has been shown to be dysregulated and be associated with poorer disease-specific survival in some cancers (18–22). But the role of miR-483 in lung cancer metastasis and the molecular mechanisms by which miR-483 regulates lung cancer metastasis are not known. Here, we demonstrate that upregulation of miR-483-5p in human

Authors' Affiliations: ¹Department of Cell Biology, School of Basic Medical Sciences; and ²Institute of Genetic Engineering, Southern Medical University, Guangzhou, China

Note: Supplementary data for this article are available at Cancer Research Online (<http://cancerres.aacrjournals.org/>).

Corresponding Author: Xiaochun Bai, Department of Cell Biology, School of Basic Medical Sciences, Southern Medical University, Guangzhou 510515, China. Phone: 86-20-6164-8724; Fax: 86-20-6164-8208; E-mail: baixc15@smu.edu.cn

doi: 10.1158/0008-5472.CAN-13-2193

©2014 American Association for Cancer Research.

lung adenocarcinoma is correlated with the progression of the tumor. miR-483-5p is activated by WNT/ β -catenin signaling to promote lung adenocarcinoma cell EMT, invasion, and metastasis through direct targeting of the Rho GDP dissociation inhibitor alpha (RhoGDI1) and activated leukocyte cell adhesion molecule (ALCAM) *in vitro* and *in vivo*. We have also shown that downregulation of RhoGDI1 enhances expression of Snail, the most important transcriptional repressor of E-cadherin, thereby promoting EMT. Our findings identify miR-483-5p as a β -catenin-activated prometastatic miRNA and provide new insights into the molecular functions of miR-483 and RhoGDI1 as well as their regulatory mechanisms in metastasis.

Materials and Methods

Cell culture

Human NSCLC cell lines A549 and PC9 were maintained in Dulbecco's Modified Eagle Medium and RPMI-1640, respectively, and supplemented with 10% FBS (Invitrogen-GIBCO) and incubated at 37°C in 5% CO₂. They had been passed for less than 6 months in culture when the experiments were carried out. Cell lines were characterized using DNA analysis by short tandem repeat fingerprinting.

Animal studies

Five-week-old female BALB/c nude mice were purchased from the Animal Center of Sun Yat-Sen University (Guangzhou, China). To evaluate *in vivo* tumor growth, 1×10^6 cells, which were suspended in 1:2 Matrigel (BD Biosciences) plus normal growth media, were injected subcutaneously into the flanks of nude mice ($n = 5$). For experimental metastasis assays, age-matched female nude mice were injected with 5.0×10^5 cells (resuspended in PBS) via the tail vein. The fluorescence emitted by cells was collected and imaged through a whole-body GFP imaging system (Lighttools). Subcutaneous tumor and lung metastases were detected by hematoxylin and eosin (H&E) staining.

Invasion and motility assays

For motility assays, 5.0×10^4 cells were placed in the top chamber of each insert (BD Biosciences) with 8.0- μ m pores; for invasion assays, 1.0×10^5 cells were seeded in a Matrigel-coated chamber (BD Biosciences). Cells were seeded in serum-free media and translocated toward complete growth media. After 24 hours of incubation at 37°C, cells that had migrated or invaded were fixed and stained in dye solution containing 20% methanol violet and 0.1% crystal. The cells that had migrated or invaded were imaged using a BH-2 inverted microscope (Olympus).

Immunoblots

Cells were lysed in 2 \times SDS sample buffer on ice and total proteins were further analyzed by SDS-PAGE and transferred to a polyvinylidene difluoride membrane, and probed with antibodies against β -actin (Santa Cruz Biotechnology, Inc.), ALCAM (Sino Biological), RhoGDI1, Fibronectin, Snail (Proteintech), N-cadherin (Epitomics), E-cadherin, and β -catenin (Cell Signaling Technology). After incubation with primary

antibodies, the membranes were washed with TBS/0.05% Tween-20 and incubated with horseradish peroxidase-conjugated secondary antibodies at room temperature for 1 hour. Proteins were detected by enhanced chemiluminescence substrates (PerkinElmer).

Rac1/cdc42 activation assay

Cells were harvested in magnesium-containing lysis buffer 3 days after transfection, and the lysates were sonicated for 5 seconds and centrifuged for 30 minutes at $18,000 \times g$ and 4°C following the manufacturer's specifications for the Rac/Cdc42 Assay Reagent Kit (Upstate Biotechnology, Inc.). A total of 10 μ g Rac/Cdc42 assay reagent was added to 600 μ L protein lysate and gently rocked at 4°C for 30 minutes. PAK-21-agarose conjugates were collected by centrifugation for 5 seconds at $14,000 \times g$ at room temperature and washed three times with 500 μ L magnesium-containing lysis buffer, and bound protein was eluted in 25 μ L SDS-PAGE sample buffer. Western blotting of these samples and of 10 μ L of the original lysate as a loading control was performed using standard protocols.

Luciferase assays

A total of 5.0×10^4 A549 cells were cotransfected with 50 ng of the indicated pMIR-REPORT luciferase construct and 50 ng of a pMIR-REPORT β -gal normalization control. All cells were also transfected with miR-483-5p mimics or negative control. Lysates were collected 36 hours after transfection, and β -gal and firefly luciferase activities were measured with β -gal and the Luciferase Reporter System (Promega).

miRNA detection

Total RNA, inclusive of the small RNA fraction, was extracted from cultured cells with a Tissue Total RNA Extraction Kit (GenePharma). Reverse transcription reactions were carried out using M-MLV reverse transcriptase (Invitrogen). Real-time PCR was performed on an Applied Biosystem StepOnePlus, using a SYBR Green I Real-Time PCR Kit (GenePharma) for miR-483-5p. The relative expression levels of miRNAs in each sample were calculated and quantified using the $2^{-\Delta\Delta C_t}$ method after normalization for expression of the positive control.

In situ hybridization and immunohistochemistry of human TMAs

Lung adenocarcinoma tissue microarrays (HLug-Ade150CS-1; Shanghai Outdo Biotech) were constructed with 75 formalin-fixed, paraffin-embedded lung adenocarcinoma tissues and their corresponding adjacent lung tissues. The protocol for detection of miRNAs by *in situ* hybridization (ISH) has been previously published (23). The sequences of the probes (Exiqon) for hsa-miR-483-5p containing the locked nucleic acid/digoxigenin-modified bases were as follows: CTCCTTCT-TTCCTCCGTCTT. Immunohistochemical staining for proteins was carried out as previously described (24, 25). The intensity of miR-483-5p and proteins staining in epithelial cells of the 75 lung adenocarcinoma samples was scored using a semiquantitative scale as previously described (24, 25). Shortly, immunostaining was defined as "high" if the immunoreactivity was observed in 10% or more of the cells in paraffin sections;

tumors with lower percentages of immunoreactive cells showed "low" immunostaining.

Statistical analysis

Statistical analysis was conducted using the SPSS statistical software program (Version 13.0; SPSS Inc.). The association between miR-483-5p and protein expression was analyzed by the χ^2 test. Differences between groups were analyzed using the Student *t* test and one-way ANOVA, or if the data violated a normal distribution, by the nonparametric Mann-Whitney test, and a level of *P* < 0.05 was considered statistically significant. Data are presented as mean \pm SEM unless otherwise indicated. Correlations were performed using Pearson correlation analysis.

Results

Upregulation of miR-483-5p is correlated with the progression of human lung adenocarcinoma

miR-483 has been shown to be dysregulated in some cancers recently. To identify the role of miR-483-5p in lung cancer metastasis, we first analyzed the correlation between miR-483-5p expression and clinicopathologic parameters in patients with lung adenocarcinoma based on the results from tissue microarray analysis (TMA). An ISH TMA was used in this study, which was constructed with 75 formalin-fixed, paraffin-embedded lung adenocarcinoma tissues and their corresponding adjacent lung tissues (Fig. 1A; Supplementary Fig. S1; Supplementary Table S1 and S2). The results indicated that the level of miR-483-5p in lung adenocarcinoma was markedly enhanced as compared with that in adjacent tissues (Fig. 1A; Supplementary Table S2). Most of the adjacent lung tissues (97.3%) showed low and only 2.7% showed high miR-483-5p staining, whereas 37% tumors demonstrated high miR-483-5p staining. Furthermore, miR-483-5p was significantly upregulated in malignant as compared with benign tumors. All 75 patients were divided into three groups based on clinicopathologic features associated with lymph node and distant metastases. Most of the tumors from metastasis-free patients (75.0%) showed low miR-483-5p staining, whereas most tumors (54.8%) from patients with metastases demonstrated high miR-483-5p staining. The tumors from patients with distant metastases demonstrated the strongest miR-483-5p expression, with all tumors showing high miR-483-5p staining (Fig. 1A; Supplementary Table S2). The results suggest a strong correlation between miR-483-5p and lung adenocarcinoma metastasis.

miR-483 regulates EMT and enhances the invasiveness and motility of lung adenocarcinoma cells *in vitro*

To identify the role of miR-483 in lung adenocarcinoma metastasis, we transfected lung adenocarcinoma cells A549 or PC9 with pcDNA 3.1(+)-miR-483 or the control vector. Ninety-six hours after transfection, A549 cells overexpressing miR-483 turned from round into a spindle-like mesenchymal phenotype (Fig. 1B). In addition, we visualized the actin cytoskeleton by phalloidin staining. The result demonstrated that F-actin distribution was rearranged in these cells from a cortical to a stress-fiber pattern, a hallmark of the mesenchymal phenotype (Fig. 1B). Immunofluorescent staining of these cells

for N-cadherin-revealed expression was increased, a typical marker of EMT (Fig. 1B). miR-483 also significantly reduced the E-cadherin, but increased the fibronectin levels (Fig. 1C), another hallmark of the mesenchymal phenotype. Although miR-483 can induce EMT, it has no obvious inhibitory effect on the proliferation of lung adenocarcinoma cells (Supplementary Fig. S2A and S2B), suggesting that growth arrest may not be required for miR-483-induced EMT in these cells.

The effect of miR-483 on cell motility and invasion was tested by Transwell assays. The results showed that ectopic miR-483 expression significantly promoted A549 (Fig. 1D) and PC9 (Fig. 1E) cells migration and invasion as measured by crystal violet staining. Taken together, these *in vitro* results suggest that miR-483 induces EMT and promotes cancer cell migration and invasion.

miR-483-5p, but not miR-483-3p, significantly induces EMT and promotes lung adenocarcinoma cell migration and invasion

The same hairpin RNA structure can generate mature products from each strand, termed 5p and 3p, that have different sequences and, therefore, target different mRNAs with different function (26). To determine which strand of miR-483 is involved in lung adenocarcinoma cells EMT, migration, and invasion, we introduced the synthesized miRNA mimics and inhibitor into lung adenocarcinoma cells. We found that miR-483-5p induced EMT in A549 as shown by the changes in cell morphology and F-actin distribution, whereas miR-483-3p did not (Supplementary Fig. S3). Similar to miR-483, miR-483-5p significantly reduced the E-cadherin, but increased the fibronectin and N-cadherin levels, whereas miR-483-3p did not (Fig. 1F).

We also found that miR-483-5p, but not miR-483-3p, promoted A549 and PC9 cell migration and invasion (Fig. 1G and H). Accordingly, silencing of miR-483-5p by transfection of cells with miR-483-5p inhibitors led to a significant decrease in cell migration and invasion (Fig. 1G and H). Taken together, these *in vitro* results suggest that miR-483-5p, but not miR-483-3p, induces EMT and promotes cell migration and invasion.

miR-483-5p promotes lung adenocarcinoma metastasis

Given these positive correlations between miR-483-5p levels and metastasis-relevant traits *in vitro*, we next assessed the potential of prometastatic roles for miR-483-5p *in vivo*. We engineered lung adenocarcinoma cells to stably overexpress miR-483-5p by lentivirus. As expected, ectopic miR-483-5p did not affect proliferation *in vitro* (Supplementary Fig. S2C and S2D), but did enhance invasion and motility (Fig. 2A and B). Hence, miR-483-5p enhances *in vitro* metastatic ability.

Because of its effects on *in vitro* traits associated with high-grade malignancy, we asked whether ectopic miR-483-5p could promote metastasis *in vivo*. Thus, the modified lung adenocarcinoma cells with miR-483-5p stable overexpression were injected into the flanks of nude mice. As shown in Fig. 2C, the control cells generally formed oval-shaped intracranial tumors and exhibited sharp edges when expanding as spheroids. In contrast, tumors formed by the miR-483-5p-transduced lung adenocarcinoma cells exhibited highly invasive morphology,

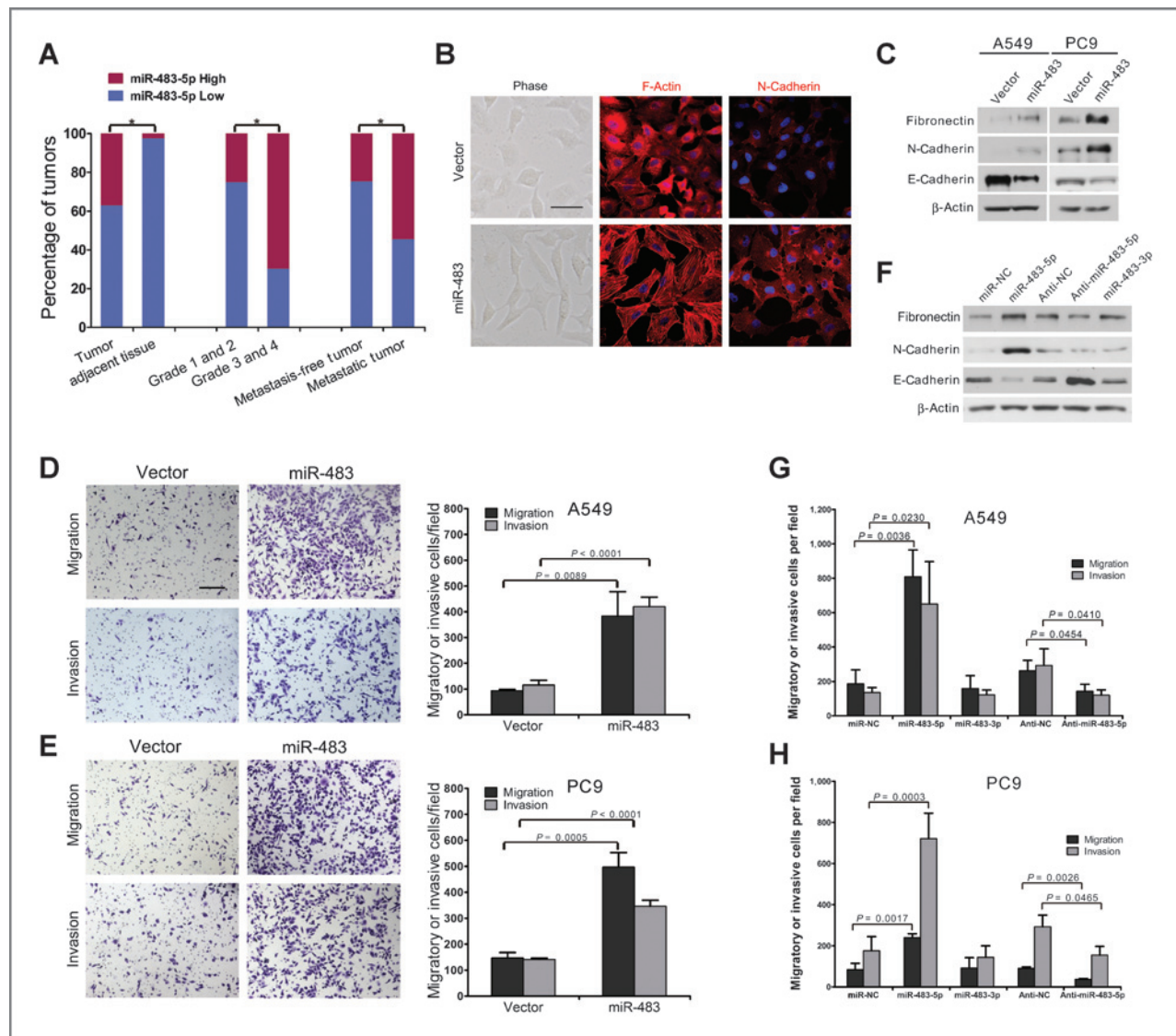


Figure 1. miR-483-5p is upregulated in human lung adenocarcinoma tissues and promotes lung adenocarcinoma cell EMT, cell motility, and invasiveness *in vitro*. **A**, the percentage of specimens showing low or high miR-483-5p expression in relation to clinicopathologic parameters. **B**, phase contrast microscopy (left), F-actin staining and N-cadherin (right) of A549 cells transfected with the miR-483-expressing vector or empty vector for 4 days. DAPI (4',6-diamidino-2-phenylindole) staining was used to detect nuclei and is merged with F-actin and N-cadherin in their respective panels; scale bars, 50 μ m. **C**, immunoblotting of fibronectin, N-cadherin, and E-cadherin in A549 and PC9 cells transfected with the miR-483-expressing vector or empty vector. β -Actin was used as a loading control. **D** and **E**, A549 and PC9 cells were transfected with the miR-483-expressing vector or empty vector and subjected to Transwell migration and invasion assays (scale bars, 100 μ m). **F**, immunoblotting of fibronectin, N-cadherin, and E-cadherin in A549 cells transfected with negative control (NC), miR-483-5p mimics, miR-483-3p mimics, anti-NC, or miR-483-5p inhibitor. β -Actin was used as a loading control. **G** and **H**, A549 and PC9 cells were transfected with NC, miR-483-5p mimics, miR-483-3p mimics, anti-NC, or miR-483-5p inhibitors and subjected to Transwell migration and invasion assays. **D**, **E**, **G**, and **H**, the results are representative of three independent experiments. Statistical analysis was performed using the Student *t* test. Right, a representative experiment is shown in triplicate (mean \pm SEM).

with the borders displaying a palisading pattern of tumor cell distribution and forming spike-like structures invading into the surrounding regions. Thus, miR-483-5p enhances local invasion. Importantly, GFP expression was maintained in the tumor cells and miR-483-5p overexpression had no obvious effect on the proliferation (Supplementary Fig. S2E).

We further determined whether the impact of miR-483-5p on metastasis was also attributable to effects on later steps of the invasion–metastasis cascade, independent of its influence

on local invasion. Thus, we injected miR-483-5p-expressing A549 cells directly into the circulation of mice, thereby circumventing the initial steps of local invasion and intravasation. Fifty-five days after tail vein injection, miR-483-5p-expressing A549 cells generated much more lung metastases than controls (Fig. 2D and E). These observations indicated that the ability of miR-483-5p-expressing cells to result in more invasive primary tumors, and to seed more metastases, is a specific consequence of the biologic activities of miR-483-5p.

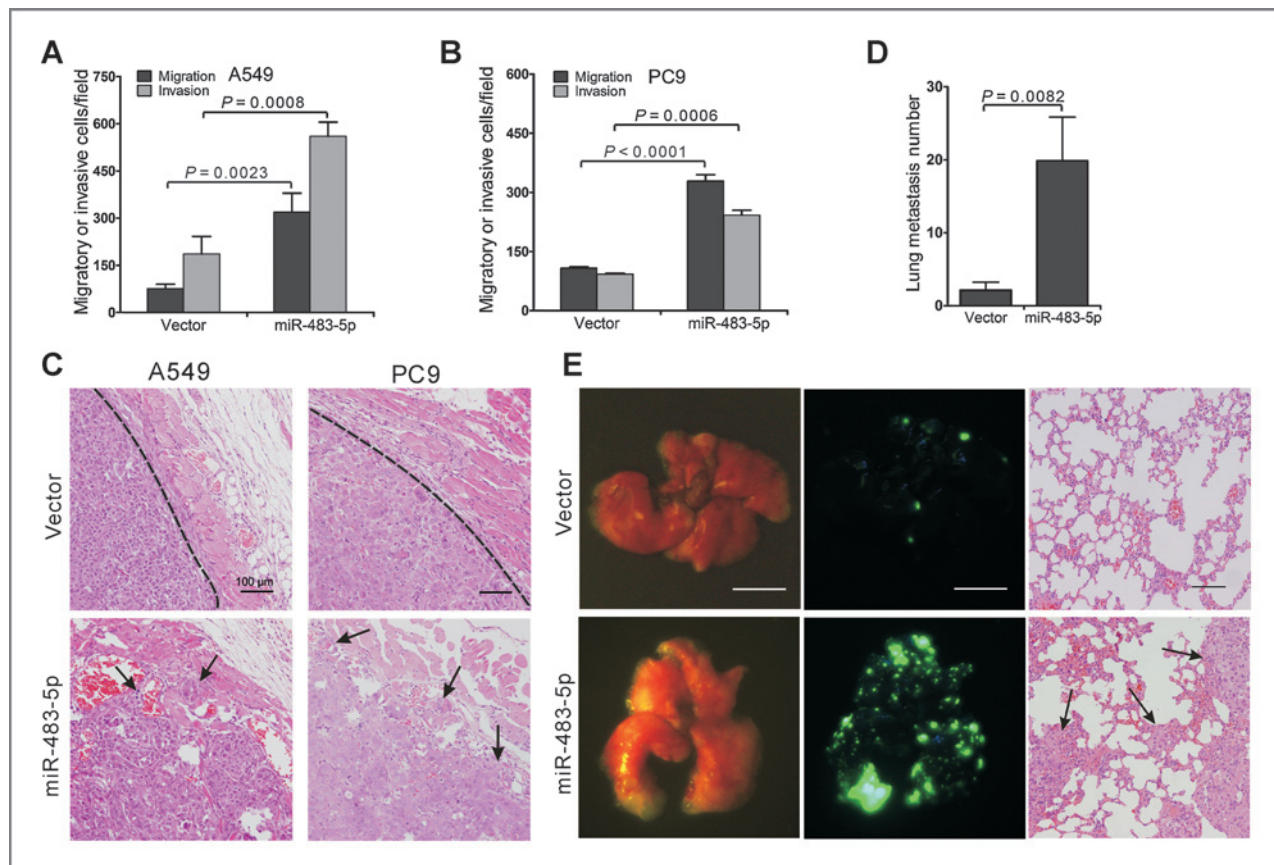


Figure 2. miR-483-5p promotes lung adenocarcinoma metastasis. A and B, Transwell migration and invasion assays of A549 and PC9 cells were performed after transduction by miR-483-expressing or vector lentivirus. C, H&E stain of miR-483-5p stable expressing A549 and PC9 primary tumors 25 days after orthotopic injection (scale bars, 100 μ m). Arrows, disseminated tumor cells in muscle or subcutis. D and E, imaging of nude mouse lungs to detect GFP-labeled A549 cells 55 days after tail vein injection (left; scale bars, 5 mm) and H&E stain of lungs (right; scale bars, 100 μ m); arrows, metastatic foci. Statistical analysis of lung metastasis was performed using the Student *t* test. Data, mean \pm SEM; *n* = 6.

Silencing of miR-483-5p inhibits lung adenocarcinoma metastasis

We next asked whether inhibition of miR-483-5p prevents the acquisition of aggressive traits. To do so, we engineered lung adenocarcinoma cells to stably inhibit miR-483-5p with a lentivirus-mediated antagomir. The results showed that suppression of miR-483-5p decreased motility and invasion (Fig. 3A and B); however, cell proliferation was unaffected *in vitro* (Supplementary Fig. S2C and S2D). Thus, miR-483-5p antagomir had the opposite effect with miR-483-5p.

We asked whether inhibition of miR-483-5p could decrease local invasion. Thus, A549 and PC9 cells with miR-483-5p inhibited were injected into the orthotopic site of nude mice. As expected, primary tumors derived from miR-483-5p antagomir-expressing cells were well encapsulated and less invasive (Fig. 3C). Furthermore, inhibition of miR-483-5p failed to alter *in vivo* proliferation and primary tumor growth (Supplementary Fig. S2F).

Then, we asked whether loss of miR-483-5p activity also inhibits metastasis by intervening at steps of the invasion-metastasis cascade subsequent to local invasion. Thus, we intravenously injected mice with miR-483-5p antagomir-

expressing A549 cells. Strikingly, miR-483-5p antagomir-expressing A549 cells metastasized to the lungs were largely devoid; cells with impaired miR-483-5p activity formed fewer lesions than controls (Fig. 5D and E).

Together, these data extended and reinforced our ectopic expression studies by demonstrating that miR-483-5p affects local invasion, early post-intravasation events, and metastatic colonization.

miR-483-5p directly targets the *RhoGDI1* and *ALCAM* 3'UTR

The ability of miR-483-5p to promote multiple steps of the invasion-metastasis cascade might derive from its ability to regulate genes involved in diverse aspects of metastatic dissemination. We used two strategies to identify the effectors of miR-483-5p. On the one hand, we applied two algorithms that predict the mRNA targets of a miRNA-PicTar (27) and TargetScan (28). On the basis of the representation of miR-483-5p sites in their 3' untranslated regions (UTR), >100 mRNAs were predicted to be regulated by miR-483-5p. Among these candidates, seven genes (*ALCAM*, *FOXJ2*, *FOXO3*, *RhoGDI1*, *NDRG2*, *SOX11*, and *TFAP2B*) were

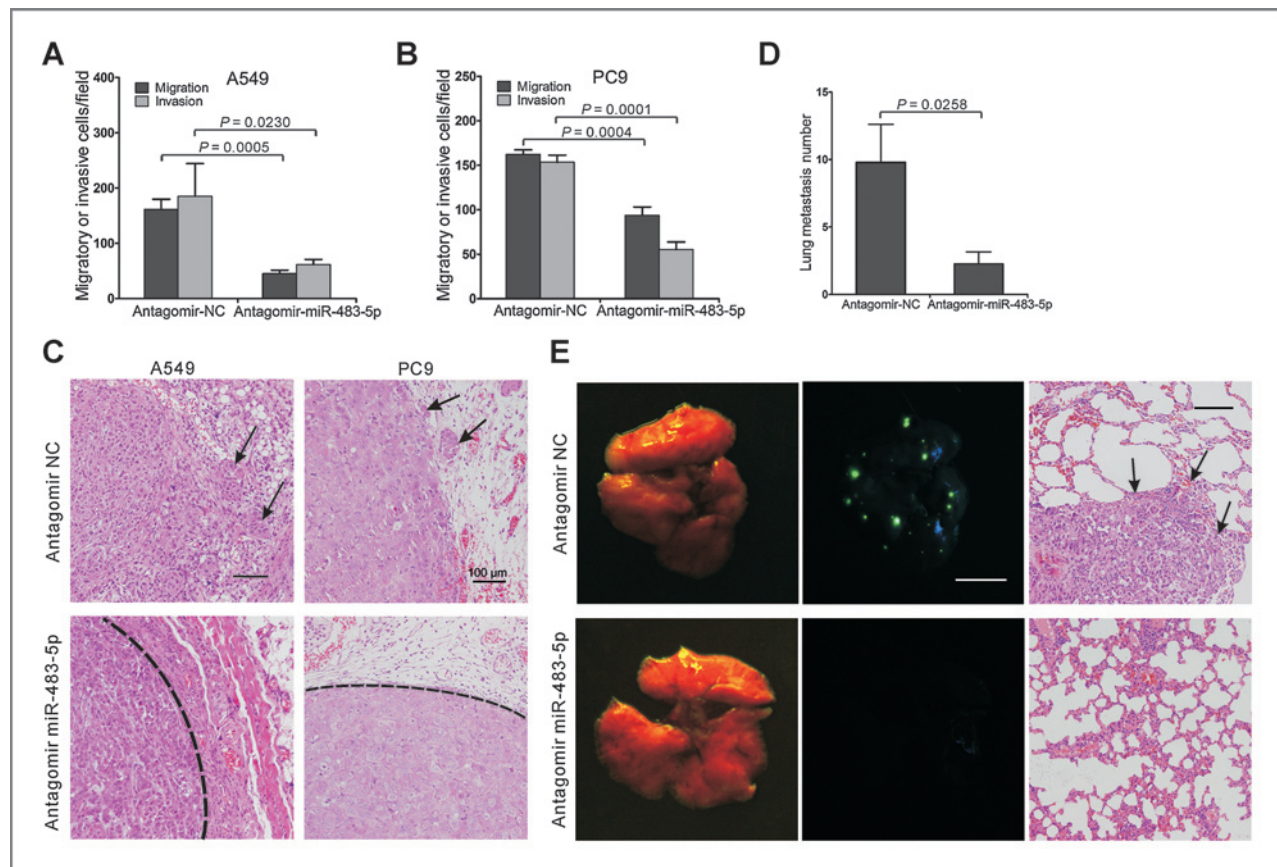


Figure 3. Silencing of miR-483-5p inhibits metastasis. **A** and **B**, Transwell migration and invasion assays of A549 and PC9 cells were performed after transduction by miR-483-inhibiting or vector lentivirus. **C**, H&E stain of antagomir miR-483-5p stable expressing A549 and PC9 primary tumors 30 days after orthotopic injection (scale bars, 100 μ m). Arrows, disseminated tumor cells in subcutis. **D** and **E**, imaging of nude mouse lungs to detect GFP-labeled A549 cells 65 days after tail vein injection (left; scale bars, 5 mm) and H&E stain of lungs (right; scale bars, 100 μ m); arrows, metastatic foci. Statistical analysis was performed using the Student *t* test; data, mean \pm SEM; *n* = 6.

involved in the suppression of cancer metastasis. On the other hand, we applied a proteomic approach using two-dimensional gel electrophoresis to identify proteins suppressed upon enhanced miR-483-5p expression in A549 cells (Fig. 4B and Supplementary Fig. S4). The putative tumor suppressors RhoGDI1 and ALCAM emerged as the most strongly downregulated proteins (Fig. 4B).

To determine whether miR-483-5p targets these genes directly, we cloned the 3'UTRs of seven putative miR-483-5p targets into a luciferase construct. Reporter assays using miR-483-5p-expressing A549 cells revealed that miR-483-5p repressed two of the UTRs: *ALCAM*, *RhoGDI1* (Fig. 4A). Mutations of the putative miR-483-5p site(s) in these two 3'UTRs abrogated responsiveness to miR-483-5p (Fig. 4C–E). In the case of *RhoGDI1*, in which 3'UTR contains two putative miR-483-5p sites, mutation of either motif can not fully abolish miR-483-5p responsiveness. Mutation of the two sites completely abolished the ability of miR-483-5p to inhibit luciferase activity. These results suggest that both of these predicted sites contribute equally to miR-483-5p-mediated RhoGDI1 reduction.

In accordance with these results, we observed a clear decrease in endogenous RhoGDI1 and ALCAM protein in lung

adenocarcinoma cells with miR-483 overexpression (Fig. 4F). Furthermore, overexpression of miR-483-5p, but not miR-483-3p, significantly decreased the expression levels of RhoGDI1 and ALCAM protein (Fig. 4F). Inhibition of miR-483-5p significantly increased the expression levels of RhoGDI1 and ALCAM protein in A549 cells. Taken together, these results suggest that miR-483 can downregulate RhoGDI1 and ALCAM expression by directly targeting their 3'UTR.

Exogenous expression of miR-483-5p enhances the activation of Rac and Cdc42

Given that RhoGDI1 is the negative regulator of Rho GTPases such as Rac1 and Cdc42, we next determined whether miR-483-5p expression changes the activities of Rac and Cdc42 GTPases. As the PAK-21 protein binds to only activated (GTP-bound) forms of active GTPases, we used a PAK-21 pull-down approach to assay GTPase activity upon transfection of miR-483-5p mimics. Amounts of GTP-bound Rac1 and Cdc42 were determined by SDS-PAGE followed by immunoblotting by using published methodologies (29). As seen in Fig. 4G, transfection of miR-483-5p mimics markedly increased the amount of active Rac1 and Cdc42, whereas the protein levels of these Rho GTPases were not altered.

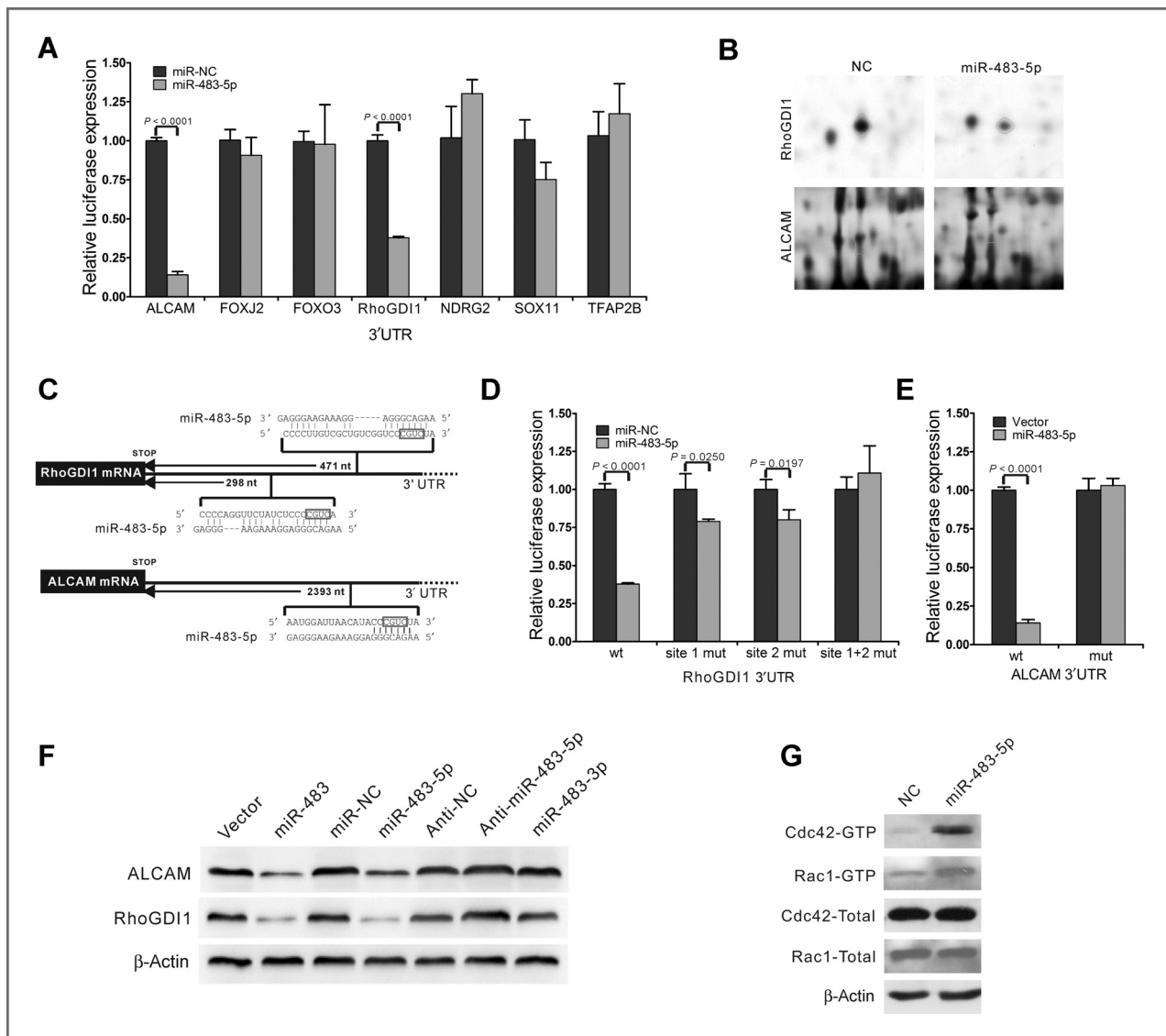


Figure 4. miR-483-5p directly targets the RhoGDI1 and ALCAM 3'UTR. **A**, Luciferase activity in A549 cells transfected with miR-483-5p mimics or negative control (NC) after transfection of the indicated 3'UTR-driven reporter constructs; $n = 3$. **B**, A549 cells were transfected with either miR-483-5p mimics or negative control, harvested after 48 hours, and identified the putative miR-483-5p target genes by 2D-DGE. Enlarged area maps of spots (corresponding to ALCAM and RhoGDI1). **C**, the putative miR-483-5p-binding site in the RhoGDI1 and ALCAM 3'UTR; nt, nucleotides. **D** and **E**, luciferase activity in the indicated A549 cells upon transfection of miR-483-5p site mutant 3'UTR-driven reporter constructs; wt, wild-type; site 1, the miR-483-5p motif at nt 317–320 of the RhoGDI1 3'UTR; site 2, the motif spanning nt 492–495; $n = 3$. **F**, the protein levels of RhoGDI1 and ALCAM were determined by Western blot analyses after transfection with miR-483 or vector plasmid, or transfection with miR-483-5p mimics, miR-483-3p mimics, negative control, anti-miR-483-5p, or anti-NC in A549 cells. **G**, the activities and protein levels of Rac1 and Cdc42 in A549 cells were determined after transfection with miR-483-5p or negative control. β -Actin served as a loading control.

miR-483-5p overexpression and RhoGDI1 inhibition produce similar changes, which are rescued by RhoGDI1 ectopic expression *in vitro*

We further found that knockdown of RhoGDI1 produced similar changes in invasion and motility assay to that of miR-483-5p overexpression, whereas knockdown of ALCAM promoted invasion less effectively (Fig. 5A–D). To determine whether these effects depend specifically on RhoGDI1 or ALCAM suppression, we used an expression construct that encodes the entire RhoGDI1 or ALCAM coding sequence but lacks the 3'UTR. Ectopic expression of ALCAM with this

construct partially rescued miR-483-5p-mediated invasion in miR-483-5p-overexpressing cells (Fig. 5B and D). Surprisingly, reexpression of RhoGDI1 completely inhibited miR-483-5p-mediated invasion (Fig. 5A and C). This suggests that, after miR-483-5p overexpression, a decrease in RhoGDI1 is required for cells to show increased invasiveness.

Then we ask whether RhoGDI1 or ALCAM connects miR-483-5p and EMT. Interestingly, A549 cells changed from round to a spindle-like mesenchymal phenotype after knockdown of RhoGDI1 (Fig. 5E), which mimic the effect of miR-483-5p on EMT, whereas ALCAM did not (Supplementary Fig. S5).

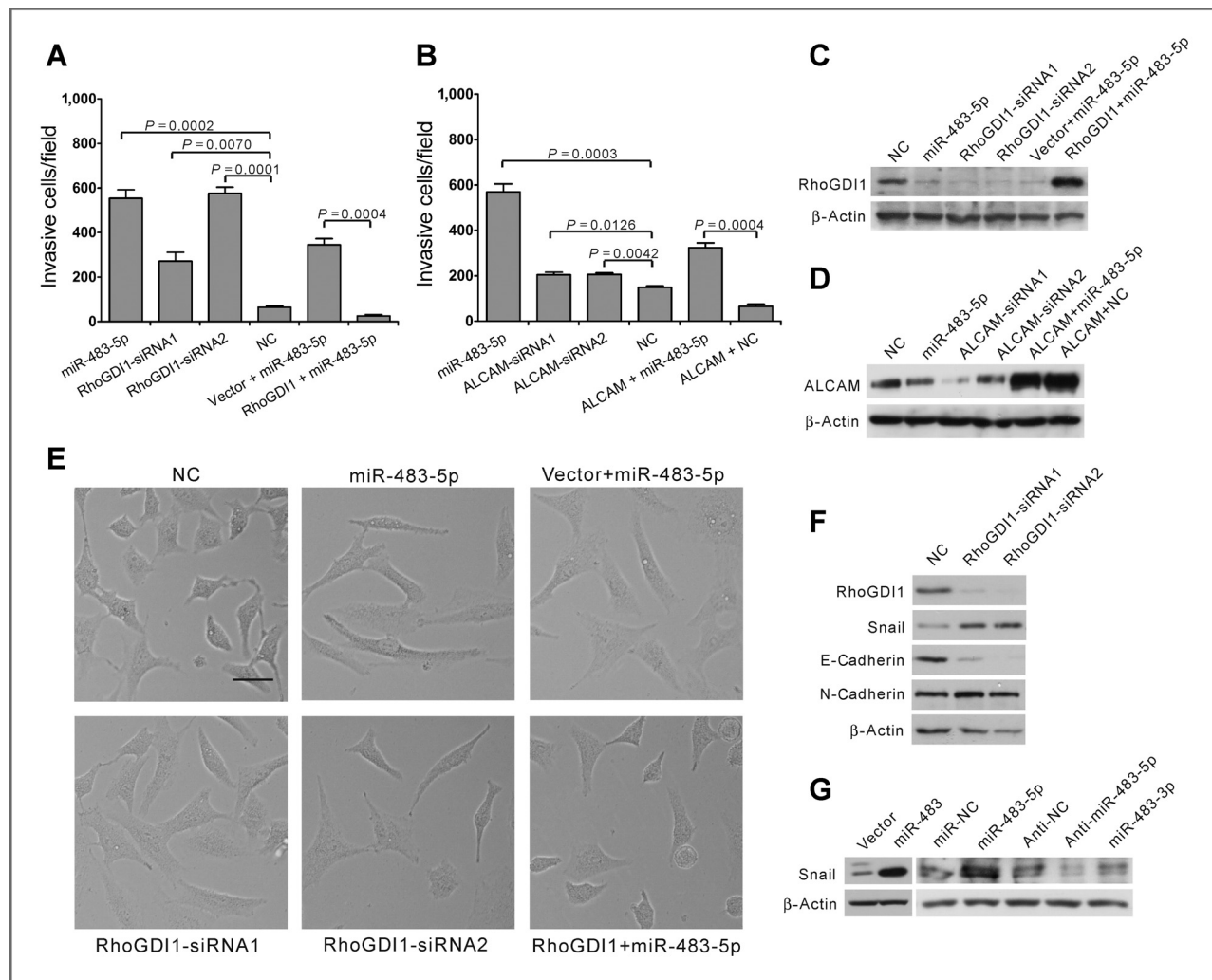


Figure 5. miR-483-5p overexpression and RhoGDI1 inhibition produce similar changes, which are restored by RhoGDI1 ectopic expression *in vitro*. A, Transwell invasion assays of A549 cells were performed after transfection with negative control (NC), siRNA against RhoGDI1, and/or miR-483-5p as indicated. B, Transwell invasion assays of A549 cells were performed after transfection with negative control, siRNA against ALCAM, and/or miR-483-5p as indicated. The results are representative of at least three independent experiments. Statistical analysis was performed using the Student *t* test. C and D, RhoGDI1 and ALCAM protein were detected by Western blot analysis. E, phase contrast microscopy of A549 cells transfected as indicated (scale bars, 50 μ m). F, A549 cells were transfected with RhoGDI1 siRNAs, then RhoGDI1, Snail, E-cadherin, and N-cadherin protein levels were detected by Western blot analysis. β -Actin served as an internal control. G, A549 cells were transfected with negative control, miR-483-5p mimics, miR-483-3p mimics, anti-NC or miR-483-5p inhibitor, and Snail was then detected by Western blot analysis.

Furthermore, knockdown of RhoGDI1 also significantly reduced the E-cadherin, but increased the N-cadherin levels (Fig. 5F).

The loss of E-cadherin is the hallmark of EMT. Several transcription factors have been implicated in the transcriptional repression of E-cadherin. Snail is the first discovered and most important transcriptional repressor of E-cadherin (30). Furthermore, snail was found to promote tumor progression in NSCLC (31). Surprisingly, we found that Snail was upregulated by miR-483-5p and downregulated by anti-miR-483-5p (Fig. 5G). Given that RhoGDI1 may connect miR-483-5p and EMT, we ask whether RhoGDI1 connects miR-483-5p and Snail. Interestingly, knockdown of RhoGDI1 produced a similar change in Snail expression to that of miR-483-5p (Fig. 5F). Taken together, these data indicated that the ability of miR-

483-5p to promote metastasis is attributable, in significant part, to its capacity to inhibit RhoGDI1.

miR-483-5p is regulated by WNT/ β -catenin signaling in lung adenocarcinoma cells

It has been reported that miR-483 expression in colon cancer cells can be driven by β -catenin (32). To further confirm these results in lung adenocarcinoma cell, we stabilized β -catenin protein by treating A549 cells with lithium chloride (LiCl), an inhibitor of GSK3 β , which is responsible for β -catenin degradation. It was found that the expression of the miR-483-5p was significantly activated by LiCl treatment (Fig. 6A). Furthermore, we transiently knocked down β -catenin in A549 cells. Quantitative real-time PCR (qRT-PCR) verified a significant

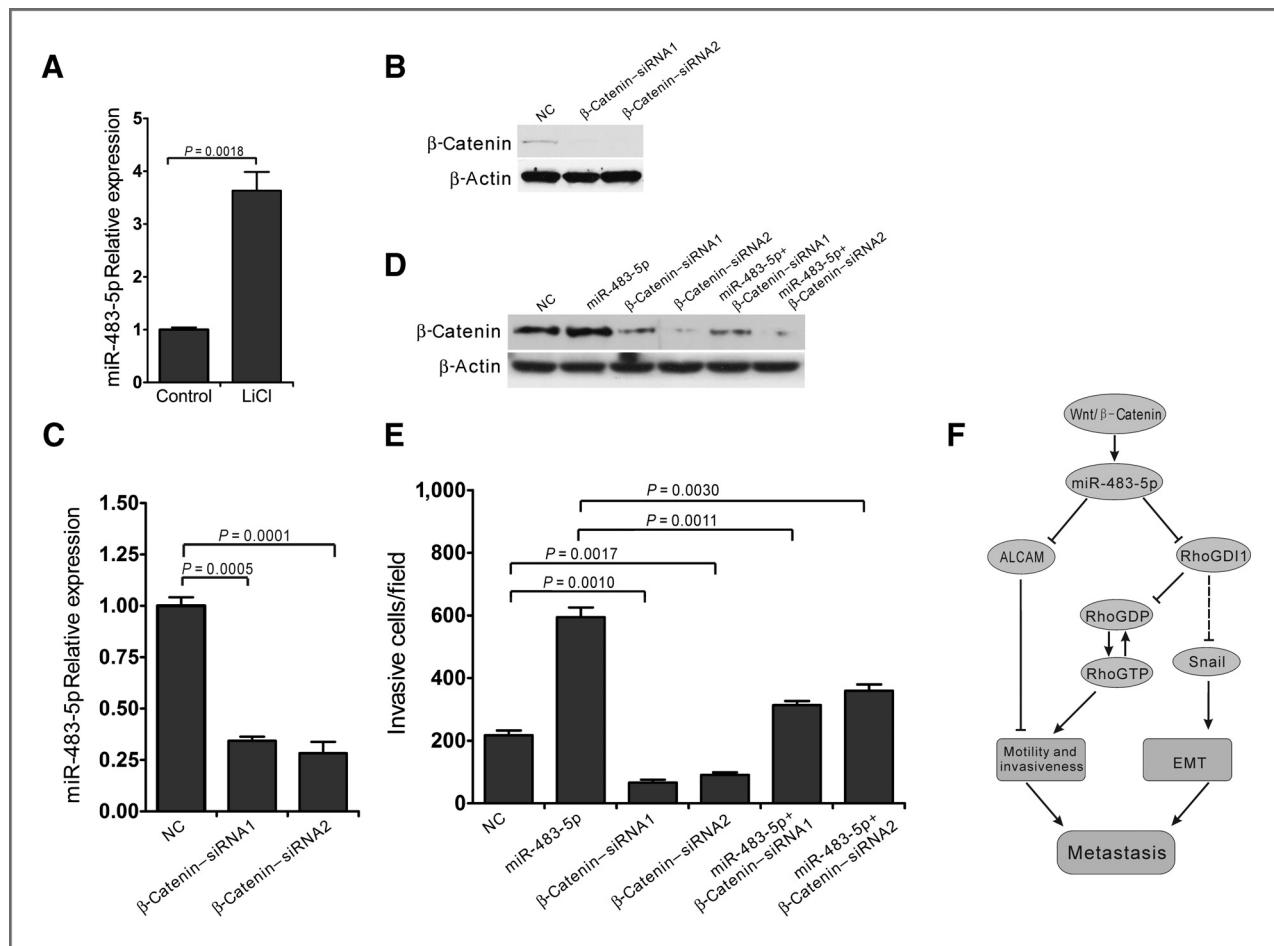


Figure 6. Regulation of miR-483-5p by the β -catenin reveals a novel mechanism by which Wnt/ β -catenin signaling contributes to cancer metastasis. A, qRT-PCR analysis of miR-483-5p in A549 cells treated with or without LiCl (20 mmol/L) for 36 hours. B and C, qRT-PCR analysis of miR-483-5p and Western blot analysis of β -catenin protein levels in A549 cells transfected with negative control (NC) or siRNAs against β -catenin. qRT-PCR data were normalized using U6 RNA. Experiments were performed three times, and the data are presented as the mean \pm SEM. Statistical analysis was performed with the Student *t* test. D and E, Transwell invasion assays and Western blot analysis of β -catenin were performed in A549 cells transfected with negative control, miR-483-5p mimics, and/or siRNAs against β -catenin. F, graphical representation illustrating the role of the miR-483-5p-mediated pathway in lung adenocarcinoma metastasis.

reduction of miR-483-5p expression in cells transfected with β -catenin siRNA (Fig. 6B and C).

It is reported that knockdown of β -catenin decreases the invasiveness of cancer cell (33). The invasion assay results showed that knockdown of β -catenin decreased the invasiveness of A549 cells (Fig. 6D and E). Furthermore, reexpression of miR-483-5p restored the decreased invasiveness of A549 cells. Taken together, these results suggest that miR-483-5p expression can be driven by WNT/ β -catenin signaling, and may play a role in WNT/ β -catenin-mediated metastasis.

Clinical associations of miR-483-5p with RhoGDI1, ALCAM, and β -catenin expression

We next determined whether there was an association between the expression levels of miR-483-5p and its targets in human lung adenocarcinoma tissues. It was found that miR-483-5p levels were negatively correlated with the levels of RhoGDI1 and ALCAM (Fig. 7A and B). Furthermore, we analyzed the association between RhoGDI1/ALCAM expression

and tumor grades and metastasis, and the results revealed a negative correlation between RhoGDI1/ALCAM and tumor grades (Supplementary Table S3). These results further implicate that miR-483-5p plays an important role in lung adenocarcinoma metastasis by targeting RhoGDI1 and ALCAM.

To demonstrate the relationship between WNT/ β -catenin signaling and miR-483-5p in clinical samples, we further examined the β -catenin expression in lung cancer by performing immunohistochemical staining in these clinical samples (Fig. 7; Supplementary Table S2). Interestingly, our results showed a positive correlation between miR-483-5p and β -catenin.

Collectively, our findings indicate that WNT/ β -catenin signaling-regulated miR-483-5p and its targets play a part in primary tumor formation and the metastatic process.

Discussion

On the basis of our results, we propose that miR-483-5p, which was upregulated by WNT/ β -catenin signaling, promotes EMT and lung adenocarcinoma metastasis through direct

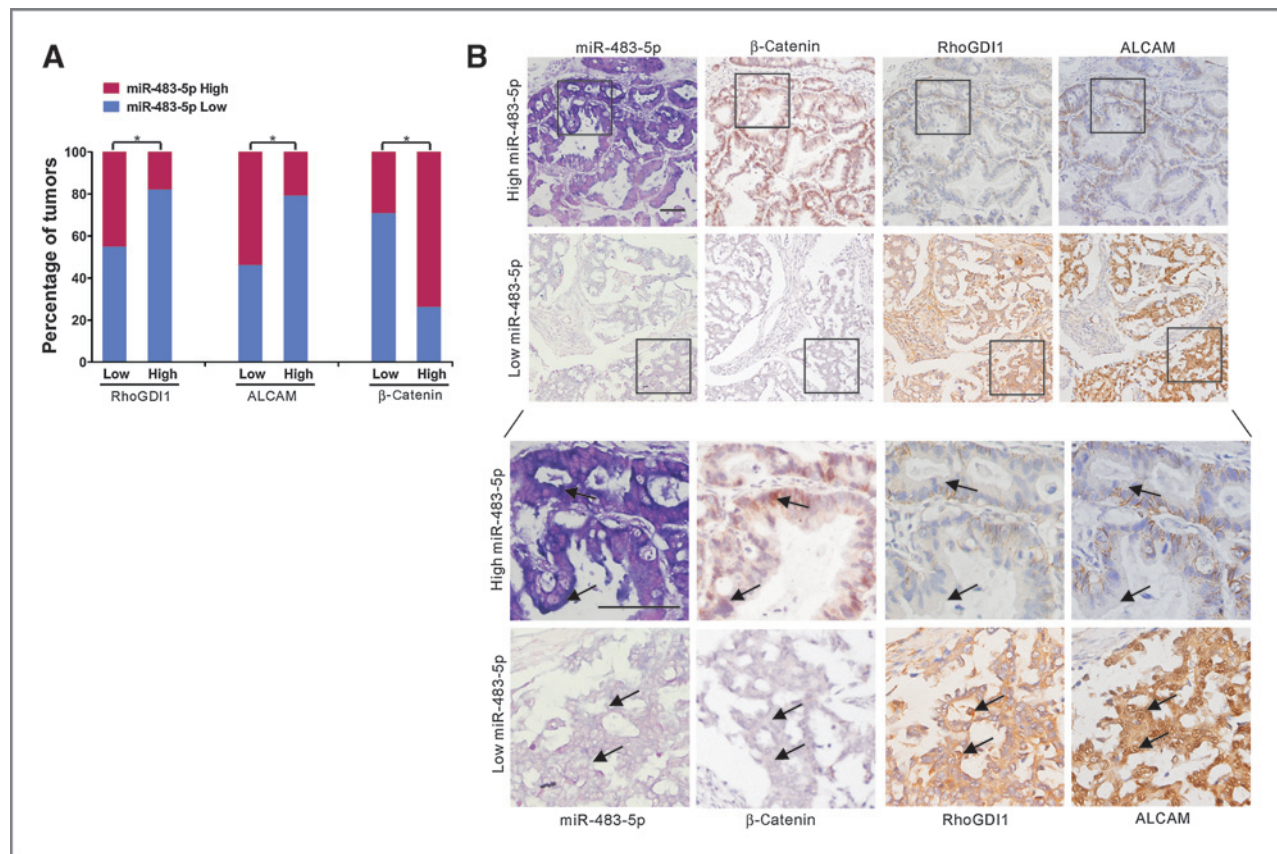


Figure 7. Clinical associations of miR-483-5p with RhoGDI1, ALCAM, and β -catenin expression. A, the percentage of specimens showing low or high miR-483-5p expression in relation to the expression levels of β -catenin, RhoGDI1, and ALCAM; *, $P < 0.05$. B, two representative cases are shown (scale bars, 100 μ m). Arrows, levels of miR-483-5p are correlated with β -catenin, RhoGDI1, and ALCAM.

targeting of RhoGDI1 and ALCAM *in vitro* and *in vivo*. Moreover, we found that downregulation of RhoGDI1, a direct and functional target of miR-483-5p, can markedly increase Snail expression, thereby promoting EMT. These findings provide new insights into the molecular functions of miR-483 as well as the role of RhoGDI1 in metastasis.

Lung cancer is the most common cause of cancer-related mortality in men and women worldwide. NSCLC accounts for 70% to 80% of lung cancer diagnoses and the disease is generally diagnosed at an advanced stage. Distant metastases, rather than the primary tumors from which these lesions arise, are responsible for >90% of carcinoma-associated mortality (1). Up to date, the molecular mechanisms underlying the development of lung cancers are still poorly understood. Therefore, a better understanding of the molecular mechanisms involved in tumor formation and development will be helpful to develop novel therapeutic targets and strategies for the treatment of human lung cancers.

miR-483 was first identified in human fetal liver (34). Recently, miR-483 has been shown to be dysregulated and associated with poorer disease-specific survival in some cancers (18–22). Despite the oncogenic role of miR-483 has been implicated by previous studies, the role of miR-483 in tumor metastasis and molecular mechanisms through which miR-483

regulates metastasis are not known. Here, we show that miR-483-5p was upregulated in lung adenocarcinoma, and, moreover, its expression levels were higher in malignant than benign tumors. And we identified miR-483 as a prometastatic miRNA and a negative regulator of the key metastasis suppressors RhoGDI1 and ALCAM.

The dysregulation of the Wnt/ β -catenin pathway has been observed in various forms of cancers. It has been recently shown that altered β -catenin expression, or WNT1, WNT3A, and WNT5A overexpression, are associated with poor prognosis in patients with NSCLC (6–9). hsa-mir-483 is located within intron 2 of the IGF2 gene. In colon cancer cells, miR-483 locus expression can be driven by β -catenin independently from IGF2 (32). Here, we demonstrate that Wnt/ β -catenin signaling activates miR-483-5p to promote EMT and enhance the invasiveness and motility of lung adenocarcinoma cells. Specifically, it is miR-483-5p, but not miR-483-3p, that significantly induces EMT and promotes lung adenocarcinoma cell migration and invasion. Therefore, this study revealed a novel mechanism by which Wnt/ β -catenin signaling contributes to cancer metastasis.

Rho GTPases contribute to multiple cellular processes that could affect cancer progression, including cytoskeletal dynamics, cell adhesion, and migration (35). Rho GTPases are

activated by the exchange of bound GDP for ambient GTP, which is stimulated by guanine nucleotide exchange factors (GEF) and are inactivated by hydrolysis of bound GTP to GDP catalyzed by GTPase-activating proteins (GAP; 36). This activity cycle is regulated by GDIs, which act to sterically shield the Rho GTPases from the action of GEFs and GAPs (37, 38). Recent studies indicate that RhoGDI1 functions as a candidate metastasis suppressor, which is frequently downregulated in hepatocellular carcinoma and breast cancer (37, 38). Our findings showed that RhoGDI1 is a direct and functional target for miR-483-5p, which can directly suppress RhoGDI1 expression and, thus, in turn activate Rac1 and Cdc42. Downregulation of RhoGDI1 by miR-483-5p increases cell motility and invasiveness and contributes to metastases formation. Furthermore, we found that downregulation of RhoGDI1 induced the expression of Snail, and thereby promoted EMT. The regulation of EMT by RhoGDI1 has not been reported in previous studies. These findings further establish RhoGDI1 as a critical metastasis suppressor.

ALCAM is involved in both homotypic and heterotypic (to lymphocyte cell surface receptor CD6) adhesion (39). It has been implicated in pathologic states, such as cancer metastasis, but its role remains inconsistent. ALCAM was found to be upregulated in melanoma, colon cancer, esophageal squamous cell carcinoma, and gastric cancer and plays a role in promoting motility and migration (40–43). In prostate carcinoma, ALCAM was upregulated in low-grade tumors, but downregulated in high-grade tumors (44). In this study, we discovered that ALCAM was downregulated and targeted by miR-483-5p in human lung adenocarcinoma. Furthermore, transfection of mimics of miR-483-5p and knockdown of ALCAM significantly increased the migration of lung adenocarcinoma cells. Interestingly, we found a negative correlation between ALCAM and lung tumor grades. Considering our own and these previous published findings, it is tempting to speculate that miR-483-5p-dependent changes in ALCAM could contribute to the invasion and metastasis of cancer cells.

In the present study, we demonstrated the roles and mechanism of miR-483 in lung adenocarcinoma metastasis. Our findings identify a mechanism for downregulating RhoGDI1

and ALCAM, and indicate that elevated expression of miR-483, which is upregulated by WNT/ β -catenin signaling, contributes to EMT and metastasis. As shown by other researchers, downregulation of ALCAM and RhoGDI1 increases cancer cells motility and invasiveness. In addition, we found that downregulation of RhoGDI1 enhances the induction of Snail and promotes EMT. Thus, we reason that the role of RhoGDI1 in metastasis may be more profound than previously thought. This study also revealed a novel mechanism by which Wnt/ β -catenin signaling contributes to cancer metastasis. Because distant metastases are responsible for patient mortality in the vast majority of human carcinomas, the ability of miR-483 to impede metastasis may prove clinically useful.

Disclosure of Potential Conflicts of Interest

No potential conflicts of interest were disclosed.

Authors' Contributions

Conception and design: Q. Song, Z. Chen, X. Bai

Development of methodology: Q. Song, Y. Xu, Z. Chen, C. Jia, J. Chen, P. Lai, X. Zhou

Acquisition of data (provided animals, acquired and managed patients, provided facilities, etc.): Q. Song, Y. Xu, X. Fan

Analysis and interpretation of data (e.g., statistical analysis, biostatistics, computational analysis): Q. Song, Y. Xu

Writing, review, and/or revision of the manuscript: Q. Song, X. Bai

Administrative, technical, or material support (i.e., reporting or organizing data, constructing databases): Q. Song, C. Yang, J. Chen, Y. Zhang, P. Lai, J. Lin, M. Li

Study supervision: W. Ma, S. Luo, X. Bai

Acknowledgments

The authors thank Prof. Xiquan Han from the Department of Pathology for contributive suggestions.

Grant support

This work was supported by the State Key Development Program for Basic Research of China (2013CB945203), National Natural Sciences Foundation of China (81270088, 31271271), the Program for Changjiang Scholars and Innovative Research Team in University (IRT1142), and "Outstanding Leadership Grant" from Guangdong Province (C1030925)

The costs of publication of this article were defrayed in part by the payment of page charges. This article must therefore be hereby marked *advertisement* in accordance with 18 U.S.C. Section 1734 solely to indicate this fact.

Received August 5, 2013; revised March 4, 2014; accepted March 20, 2014; published OnlineFirst April 7, 2014.

References

- Gupta GP, Massague J. Cancer metastasis: building a framework. *Cell* 2006;127:679–95.
- Thiery JP, Acloque H, Huang RYJ, Angela Nieto M. Epithelial–mesenchymal transitions in development and disease. *Cell* 2009;139:871–90.
- Kalluri R, Weinberg RA. The basics of epithelial–mesenchymal transition. *J Clin Invest* 2009;119:1420–8.
- Anastas JN, Moon RT. WNT signalling pathways as therapeutic targets in cancer. *Nat Rev Cancer* 2013;13:11–26.
- Yook JI, Li XY, Ota I, Hu C, Kim HS, Kim NH, et al. A Wnt-Axin2–GSK3 beta cascade regulates Snail1 activity in breast cancer cells. *Nat Cell Biol* 2006;8:1398.
- Nakashima T, Liu D, Nakano J, Ishikawa S, Yokomise H, Ueno M, et al. Wnt1 overexpression associated with tumor proliferation and a poor prognosis in non–small cell lung cancer patients. *Oncol Rep* 2008;19:203–9.
- Nguyen DX, Chiang AC, Zhang XHF, Kim JY, Kris MG, Ladanyi M, et al. WNT/TCF signaling through LEF1 and HOXB9 mediates lung adenocarcinoma metastasis. *Cell* 2009;138:51–62.
- Woenckhaus M, Merk J, Stoehr R, Schaeper F, Gaumann A, Wiebe K, et al. Prognostic value of FHIT, CTNNB1, and MUC1 expression in non–small cell lung cancer. *Hum Pathol* 2008;39:126–36.
- Choi YS, Shim YM, Kim S-H, Son DS, Lee H-S, Kim GY, et al. Prognostic significance of E-cadherin and beta-catenin in resected stage I non–small cell lung cancer. *Eur J Cardiothorac Surg* 2003;24:441–9.
- Ma L, Young J, Prabhala H, Pan E, Mestdagh P, Muth D, et al. miR-9, a MYC/MYCN-activated microRNA, regulates E-cadherin, and cancer metastasis. *Nat Cell Biol* 2010;12:247–.
- Valastyan S, Reinhardt F, Benaich N, Calogrias D, Szasz AM, Wang ZC, et al. A pleiotropically acting microRNA, miR-31, inhibits breast cancer metastasis. *Cell* 2009;137:1032–46.

12. Akao Y, Nakagawa Y, Naoe T. MicroRNA-143 and -145 in colon cancer. *DNA Cell Biol* 2007;26:311–20.
13. Ma L, Teruya-Feldstein J, Weinberg RA. Tumour invasion and metastasis initiated by microRNA-10b in breast cancer. *Nature* 2007;449:682–8.
14. Tavazoie SF, Alarcon C, Oskarsson T, Padua D, Wang Q, Bos PD, et al. Endogenous human microRNAs that suppress breast cancer metastasis. *Nature* 2008;451:147–52.
15. Gregory PA, Bert AG, Paterson EL, Barry SC, Tsykin A, Farshid G, et al. The miR-200 family and miR-205 regulate epithelial to mesenchymal transition by targeting ZEB1 and SIP1. *Nat Cell Biol* 2008;10:593–601.
16. Stinson S, Lackner MR, Adai AT, Yu N, Kim H-J, O'Brien C, et al. TRPS1 targeting by miR-221/222 promotes the epithelial-to-mesenchymal transition in breast cancer. *Sci Signal* 2011;4:ra41.
17. Garzon R, Calin GA, Croce CM. MicroRNAs in cancer. *Ann Rev Med* 2009;60:167–79.
18. Wang L, Shi M, Hou S, Ding B, Liu L, Ji X, et al. MiR-483-5p suppresses the proliferation of glioma cells via directly targeting ERK1. *FEBS Lett* 2012;586:1312–7.
19. Patterson EE, Holloway AK, Weng J, Fojo T, Kebebew E. MicroRNA profiling of adrenocortical tumors reveals miR-483 as a marker of malignancy. *Cancer* 2011;117:1630–9.
20. Soon PS, Tacon LJ, Gill AJ, Bambach CP, Sywak MS, Campbell PR, et al. miR-195 and miR-483-5p identified as predictors of poor prognosis in adrenocortical cancer. *Clin Cancer Res* 2009;15:7684–92.
21. Veronese A, Lupini L, Consiglio J, Visone R, Ferracin M, Fornari F, et al. Oncogenic role of miR-483-3p at the IGF2/483 locus. *Cancer Res* 2010;70:3140–9.
22. Moussay E, Wang K, Cho JH, van Moer K, Pierson S, Paggetti J, et al. MicroRNA as biomarkers and regulators in B-cell chronic lymphocytic leukemia. *Proc Natl Acad Sci U S A* 2011;108:6573–8.
23. Dillhoff M, Liu J, Frankel W, Croce C, Bloomston M. MicroRNA-21 is overexpressed in pancreatic cancer and a potential predictor of survival. *J Gastrointest Surg* 2008;12:2171–6.
24. Camp RL, Rimm EB, Rimm DL. Met expression is associated with poor outcome in patients with axillary lymph node negative breast carcinoma. *Cancer* 1999;86:2259–65.
25. Cheng YW, Wu NF, Wang J, Yeh KT, Goan YG, Chiou HL, et al. Human papillomavirus 16/18 E6 oncoprotein is expressed in lung cancer and related with p53 inactivation. *Cancer Res* 2007;67:10686–93.
26. Almeida MI, Nicoloso MS, Zeng L, Ivan C, Spizzo R, Gafa R, et al. Strand-specific miR-28-5p and miR-28-3p have distinct effects in colorectal cancer cells. *Gastroenterology* 2012;142:886–96 e9.
27. Krek A, Grun D, Poy MN, Wolf R, Rosenberg L, Epstein EJ, et al. Combinatorial microRNA target predictions. *Nat Genet* 2005;37:495–500.
28. Grimson A, Farh KKH, Johnston WK, Garrett-Engle P, Lim LP, Bartel DP. MicroRNA targeting specificity in mammals: determinants beyond seed pairing. *Mol Cell* 2007;27:91–105.
29. Smith TK, Hager HA, Francis R, Kilkenny DM, Lo CW, Bader DM. Bves directly interacts with GEFT, and controls cell shape and movement through regulation of Rac1/Cdc42 activity. *Proc Natl Acad Sci U S A* 2008;105:8298–303.
30. Cano A, Perez-Moreno MA, Rodrigo I, Locascio A, Blanco MJ, del Barrio MG, et al. The transcription factor Snail controls epithelial-mesenchymal transitions by repressing E-cadherin expression. *Nat Cell Biol* 2000;2:76–83.
31. Yanagawa J, Walser TC, Zhu LX, Hong L, Fishbein MC, Mah V, et al. Snail promotes CXCR2 ligand-dependent tumor progression in non-small cell lung carcinoma. *Clin Cancer Res* 2009;15:6820–9.
32. Veronese A, Visone R, Consiglio J, Acunzo M, Lupini L, Kim T, et al. Mutated beta-catenin evades a microRNA-dependent regulatory loop. *Proc Natl Acad Sci U S A* 2011;108:4840–5.
33. Kobayashi T, Shimura T, Yajima T, Kubo N, Araki K, Tsutsumi S, et al. Transient gene silencing of galectin-3 suppresses pancreatic cancer cell migration and invasion through degradation of beta-catenin. *Int J Cancer* 2011;129:2775–86.
34. Fu H, Tie Y, Xu C, Zhang Z, Zhu J, Shi Y, et al. Identification of human fetal liver miRNAs by a novel method. *FEBS Lett* 2005;579:3849–54.
35. Sahai E, Marshall CJ. RHO: GTPases and cancer. *Nat Rev Cancer* 2002;2:133–42.
36. Garcia-Mata R, Boulter E, Burridge K. The 'invisible hand': regulation of RHO GTPases by RHOGEFs. *Nat Rev Mol Cell Biol* 2011;12:493–504.
37. Jiang WG, Watkins G, Lane J, Cunnick GH, Douglas-Jones A, Mokbel K, et al. Prognostic value of rho GTPases and rho guanine nucleotide dissociation inhibitors in human breast cancers. *Clin Cancer Res* 2003;9:6432–40.
38. Ding J, Huang S, Wu S, Zhao Y, Liang L, Yan M, et al. Gain of miR-151 on chromosome 8q24.3 facilitates tumour cell migration and spreading through downregulating RhoGDIa. *Nat Cell Biol* 2010;12:390–.
39. Ofori-Acquah SF, King JA. Activated leukocyte cell adhesion molecule: a new paradox in cancer. *Transl Res* 2008;151:122–8.
40. Weichert W, Knoesel T, Bellach J, Dietel M, Kristiansen G. ALCAM/CD166 is overexpressed in colorectal carcinoma and correlates with shortened patient survival. *J Clin Pathol* 2004;57:1160–4.
41. Jin Z, Selaru FM, Cheng Y, Kan T, Agarwal R, Mori Y, et al. MicroRNA-192 and -215 are upregulated in human gastric cancer *in vivo* and suppress ALCAM expression *in vitro*. *Oncogene* 2011;30:1577–85.
42. van Kempen LC, van den Oord JJ, van Muijen GN, Weidle UH, Bloemers HP, Swart GW. Activated leukocyte cell adhesion molecule/CD166, a marker of tumor progression in primary malignant melanoma of the skin. *Am J Pathol* 2000;156:769–74.
43. Verma A, Shukla NK, Deo SVS, Gupta SD, Ralhan R. MEMD/ALCAM: a potential marker for tumor invasion and nodal metastasis in esophageal squamous cell carcinoma. *Oncology* 2005;68:462–70.
44. Kristiansen G, Pilarsky C, Wissmann C, Stephan C, Weissbach L, Loy V, et al. ALCAM/CD166 is upregulated in low-grade prostate cancer and progressively lost in high-grade lesions. *Prostate* 2003;54:34–43.

Cancer Research

The Journal of Cancer Research (1916–1930) | The American Journal of Cancer (1931–1940)

miR-483-5p Promotes Invasion and Metastasis of Lung Adenocarcinoma by Targeting RhoGDI1 and ALCAM

Qiancheng Song, Yuanfei Xu, Cuilan Yang, et al.

Cancer Res 2014;74:3031-3042. Published OnlineFirst April 7, 2014.

Updated version Access the most recent version of this article at:
doi:[10.1158/0008-5472.CAN-13-2193](https://doi.org/10.1158/0008-5472.CAN-13-2193)

Supplementary Material Access the most recent supplemental material at:
<http://cancerres.aacrjournals.org/content/suppl/2014/04/14/0008-5472.CAN-13-2193.DC1.html>

Cited articles This article cites 44 articles, 11 of which you can access for free at:
<http://cancerres.aacrjournals.org/content/74/11/3031.full.html#ref-list-1>

Citing articles This article has been cited by 1 HighWire-hosted articles. Access the articles at:
<http://cancerres.aacrjournals.org/content/74/11/3031.full.html#related-urls>

E-mail alerts [Sign up to receive free email-alerts](#) related to this article or journal.

Reprints and Subscriptions To order reprints of this article or to subscribe to the journal, contact the AACR Publications Department at pubs@aacr.org.

Permissions To request permission to re-use all or part of this article, contact the AACR Publications Department at permissions@aacr.org.